

# 1 Confocal Scanning Optical Microscopy and Nanotechnology

Peter J. Lu

## 1.1 Introduction

Microscopy is the characterization of objects smaller than what can be seen with the naked human eyes, and from its inception, optical microscopy has played a seminal role in the development of science. In the 1660s, Robert Hooke first resolved cork cells and thereby discovered the cellular nature of life [1]. In 1827, Robert Brown's observation of the seemingly random movement of pollen grains [2] led to the understanding of the motion that still bears his name, and ultimately to the formulation of statistical mechanics. The contributions of optical microscopy continue into the present, even as the systems of interest approach nanometer size. What makes optical microscopy so useful is the relatively low energy of visible light: in general, it does not irreversibly alter the electronic or atomic structure of the matter with which it interacts, allowing observation of natural processes in situ. Moreover, light is cheap, abundant, and can be manipulated with common and relatively inexpensive laboratory hardware.

In an optical microscope, illuminating photons are sent into the sample. They interact with atoms in the sample, and are re-emitted and captured by a detection system. The detected light is then used to reconstruct a map of the sample. An ideal microscope would detect each photon from the sample, and measure with infinite precision the three-dimensional position from which it came, when it arrived, and all of its properties (energy, polarization, phase). An exact three-dimensional map of the sample could then be created with perfect fidelity. Unfortunately, these quantities can be known only to a certain finite precision, due to limitations in both engineering and fundamental physics.

One common high-school application of optical microscopy is to look at small objects, for example, the underside of a geranium leaf. Micron-scale structure is easily revealed in the top layer of plant cells. But structure much smaller than a micron (such as individual macromolecules in the plant cell) cannot be seen, and looking deep into the sample (e.g. tens of cell layers) leads only to a nearly featureless blur. Clearly this is a far cry from the ideal microscope above.

Microscopes with improved resolution fall into two broad categories—near-field and far-field. Near-field technique relies on scanning a nanoscale optical probe only nanometers above the surface of interest. Spatial resolution is then

physically limited only by the lateral size of the probe tip, and information can only be gathered from the surface. This technique is the subject of another chapter in this text. In far-field, a macroscopic lens (typically with mm-scale lens elements) collects photons from a sample hundreds of microns away. Standard microscopes, like the one used in high-school, are of this type. The light detected often comes from deep within the sample, not just from the surface. Moreover, there are often enough photons to allow collection times sufficiently brief to watch a sample change in real time, here defined to be the video rate of about 25 full frames per second.

But all far-field techniques encounter the fundamental physical diffraction limit, a restriction on the maximum spatial resolution. In the present parlance, the precision with which the location of the volume generating a given detected photon (here termed the illumination volume) can be determined is roughly the same size as the wavelength of that photon[3]. Visible light has a wavelength of roughly a half micron, an order of magnitude greater than the feature size of interest to nanotechnology.

At first blush, then, the idea that far-field optical microscopy can contribute much to nanotechnology may appear absurd. However, a number of techniques have been developed to improve the precision with which the spatial position of an illumination volume can be determined. The most prevalent of these is confocal microscopy, the main subject of this chapter, where the use of a pinhole can dramatically improve the ability to see small objects. Other techniques have the potential for further improvements, but none so far has been applied widely to systems relevant to nanotechnology.

Several terms are commonly used to describe the improvements in “seeing” small objects. Resolution or resolving power is the ability to characterize the distribution of sample inhomogeneities, for example, distinguishing the internal structure of cells in Hooke’s cork or the geranium leaf. Resolution is ultimately restricted by the diffraction limit: no optical technique, including confocal, will ever permit resolution of single atoms in a crystal lattice with angstrom-scale structure. On the other hand, localization is the determination of the spatial position of an object, and this is possible even when the object is far smaller than the wavelength. Localization can be of an object itself, if there is sufficient optical contrast with the surrounding area, or of a fluorescent tag attached to the object. The former is generally more common in the investigation of nanoscale materials, where in many instances (e. g. , quantum dots) the nanomaterials are themselves fluorescent. The latter is common in biology, where the confocal is often used to localize single-molecule fluorescent probes attached to cellular substructures. But in many of these systems, the tags can be imaged without confocality, such as in thin cells where three-dimensional sectioning is unneeded, or when the tags are spaced out by microns or more.

Precise localization is of tremendous utility when the length scale relevant to the question at hand is greater than the wavelength being used to probe the sample, even if the sample itself has structure on a smaller length scale. For

example, Brown observed micron-scale movements of pollen grains to develop his ideas on motion, while the nanoscale (i. e., molecular) structure of the pollen was entirely irrelevant to the question he was asking. The pollen served as ideal zero-dimensional markers that he could observe; their position as a function of time, not their structure, was ultimately important. In many instances, the confocal plays a similar role, where fluorescent objects serve as probes of other systems. By asking the right questions, the diffraction limit only represents a barrier to imaging resolution, not a barrier to gathering information and answering a properly formulated scientific question.

Ultimately, the confocal is not a fancy optical microscope that through special tricks allows resolution of nanoscale objects. Rather, the confocal makes the greatest contribution to nanotechnology with rapid, non-destructive three-dimensional nanoscale localization of the sample area generating a given detected photon, and the analysis (spectroscopy) of that photon. This localization property of the confocal allows real-time spectroscopy of individual nanoscale objects, instead of ensemble averages. As such, the confocal plays a singularly important role in the investigation of structure and dynamics of systems relevant to nanotechnology, complementing the other techniques described in this volume.

This review begins with a qualitative overview (no equations) of confocal microscopy, with a brief discussion of recent advances to improve resolution and localization. Following that is a survey of recent applications of confocal microscopy to systems of interest to nanotechnology.

## 1.2 The Confocal Microscope

### 1.2.1 Principles of Confocal Microscopy

Several texts comprehensively review the confocal microscope, how it works, and the practical issues surrounding microscope construction and resolution limitations[ 4 – 7]. This section is a brief qualitative overview to confer a conceptual understanding of what a confocal is, namely how it differs from a regular optical microscope, and why those differences are important for gaining information from structures relevant to nanotechnology. All of the applications of confocal microscopy described here rely on fluorescence. That is, the incoming beam with photons of a given wavelength hits the sample, and interactions between illumination photons and sample atoms generates new photons of a lower wavelength, which are then detected. The difference in the two wavelengths must be large enough to allow separation of illumination and detection beams by mirrors, called dichroics, that reflect light of one color and pass that of another. In practice, the separation is usually tens of nanometers or more.

The noun confocal is shorthand for confocal scanning optical microscope.

Parsing in reverse, optical microscope indicates that visible radiation is used, and confocals are often based on, or built directly as an attachment to, optical microscopes with existing technology. Unlike traditional widefield optical microscopes, where the whole sample is illuminated at the same time, in confocal a beam of laser light is scanned relative to the sample, and the only light detected is emitted by the interaction between the illuminating beam and a small sample illumination volume at the focus of the microscope objective; due to the diffraction limit, the linear extent of this volume is approximately the wavelength of light. In a confocal, light coming back from the illumination volume is focused down to a another diffraction-limited spot, which is surrounded by a narrow pinhole. The pinhole spatially filters out light originating from parts of the sample not in the illumination volume. Because it is positioned at a point conjugate to the focal point in the sample, the pinhole is said to be confocal to it, and the pinhole allows only the light from the focused spot (that is, the illumination volume) to reach the detector.

A schematic of a typical confocal is given in Fig. 1.1 (see colour figure). Light from a laser beam is reflected by a dichroic and focused onto a spot on the sample in the  $x$ - $y$  plane by the microscope objective. The optic axis is along the  $z$  direction. Light from the sample, at a lower wavelength, comes back up from the illumination volume via the objective, passes through the dichroic, and is focused onto a point, surrounded by a pinhole, that is confocal with the objective's focal point on the sample. The detected light then passes to the detector. The laser beam illuminates parts of the sample covering a range of depths, which in an ordinary microscope contribute to the detected signal, and blur the image out. This is the reason that, tens of cell layers deep, the image of the geranium is blurry. In the confocal, however, the pinhole blocks all light originating from points not at the focus of the microscope objective, so that only the light from the illumination volume is detected. This effect is also known as optical sectioning. Translating the sample relative to a fixed laser beam or moving the laser beam relative to a fixed sample, allows the point-by-point construction of full three-dimensional map of the sample itself, with resolution limited by the size of the excitation volume, itself limited by the diffraction limit of the illuminating light.

### 1.2.2 Instrumentation

The different implementations of a confocal microscope differ primarily in how the illumination volume is moved throughout the sample. The simplest method from an optical standpoint is to keep the optics fixed, and translate the sample (Fig. 1.2(a)); modern piezo stages give precision and repeatability of several nanometers. Ideal from an image quality standpoint, as the optical path, can be highly optimized, and specific aberrations and distortions were removed, sample translation is also the slowest. Moving the piezo requires milliseconds,

precluding the full-frame imaging at 25 frame/s needed to achieve real-time speeds.

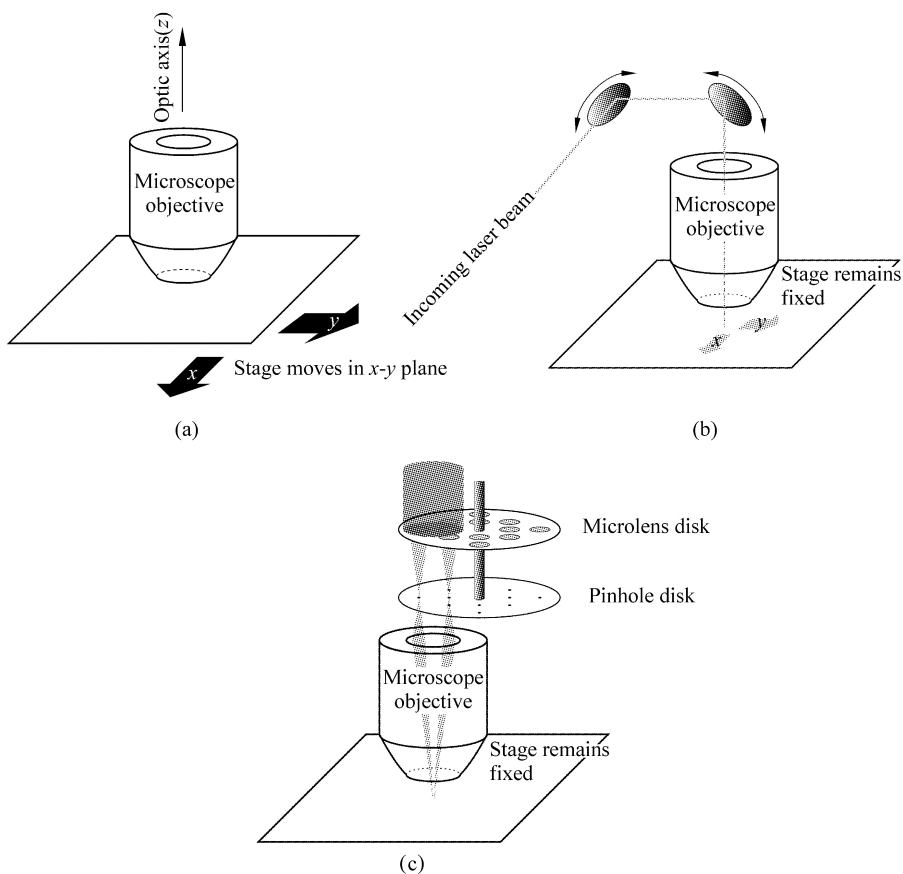


**Figure 1. 2** confocal microscope instrumentation: (a) stage-scanning, in which the optical train remains fixed and the stage is moved, (b) beam scanning, with two moveable mirrors that move the beam itself, (c) Nipkow disk, where rotating disks of microlens and pinholes parallelize the illumination beam

For higher speeds, the beam itself must be moved. Two galvanometer-driven mirrors can be used to scan the laser beam in  $x$  and  $y$  at up to a kHz, while maintaining beam quality (Fig. 1.2(b)). While not quite fast enough to achieve real-time full-frame imaging, commercial confocal microscopes based on galvanometers can reach about ten full images a second, each with about a million pixels. Beam scanning is usually accomplished much like that of a television, by first quickly scanning a line horizontally, then shifting the beam (at the end of each horizontal scan) in the vertical direction scanning another horizontal line, and so on. Replacing the galvanometer mirror that scans

horizontally with an acousto-optical device (AOD) significantly increases speed (the galvanometer is fast enough to keep up with the vertical motion). However, the AOD severely degrades the quality of the beam, and image quality correspondingly suffers. AOD-based confocals are primarily useful where gathering data at high speed is more important than achieving high resolution, as is the case in dynamical situations with relatively large (i. e., greater than micron-size) objects.

Another major approach to increasing beam-scanning speed is to split the main laser beam into thousands of smaller laser beams, parallelizing the illumination (Fig. 1. 2(c)). Each individual mini-beam then needs only to be moved a small amount in order for the total collection of beams to image an entire frame. This typically involves a Nipkow disk, where thousands of tiny microlenses are mounted in an otherwise opaque disk. These focus down to thousands of points, surrounded by thousands of tiny pinholes created in another disk. The laser light is thus split and focused, and then the multiple tiny beams are focused onto the sample with a single objective lens. Light from the multiple illumination volumes comes back up first via the objective and then through the pinholes, then goes to the camera detector, where the thousands of mini-beams are simultaneously imaged. By spinning the disk and arranging the holes in a spiral pattern, full coverage of the frame can be achieved. The main advantage of this technique is that image quality can remain high (no AOD, for instance), and speed can be increased simply by spinning the disk faster. From an engineering standpoint, Nipkow disks are durable and easy to fabricate with existing technology; their major drawback is a total lack of flexibility: Nipkow disk systems are usually optimized for only one magnification, and after fabrication, the size of the pinholes cannot be changed to accommodate different conditions.

## **1. 2. 3 Techniques for Improving Imaging of Nanoscale Materials**

### **1. 2. 3. 1 4Pi Confocal**

The biggest recent development in confocal microscopy has been the use of two objectives, focused on the same point, to collect light. The name 4Pi microscopy has been applied to this general technique, and is meant to evoke the idea that all of the light is collected from a sample simultaneously (i. e., the 4 pi steradians of a complete sphere); in reality, while most of the light is collected by the two objectives, they cannot image the whole sphere[8]. A full discussion of the principles and advances in 4Pi confocal microscopy is beyond the scope of this article ([7, 8]); only a brief qualitative discussion to convey the underlying ideas behind the superior resolution of 4Pi confocal is included here.

A regular confocal rejects light coming from parts of the sample outside of the illumination volume by means of spatial filtering through a pinhole, but even

if it is made arbitrarily small, the pinhole cannot localize the light coming from the sample to better than within the typical size of this region (i. e., the wavelength) because of diffraction. In addition, there is still a small contribution to the detected signal from light outside of the focal point, though that contribution decreases with greater distance from the focal point. Limitations to resolution therefore come from a combination of the finite size of the excitation volume in the sample, and the imperfect discrimination of the pinhole itself, both fundamental physical constraints inherent to the design of a confocal microscope; they cannot be overcome simply with better implementation of the same ideas. 4Pi confocal relies on coherent illumination or detection from both objectives simultaneously, effectively doubling amount of light involved and creating an interference pattern between the two beams. This allows a dramatic increase in axial resolution, often around five-fold, though lateral resolution is unchanged.

From an instrumentation standpoint, there are three different types of 4Pi confocal microscopes A, B and C (Fig. 1.3(see colour figure)). In type-A 4Pi confocal, illumination beams are sent through both objectives and interfere in the sample; the light coming out of only one objective is used for detection. This is the earliest and simplest system, and has thus far been most widely used. In type-B, illumination occurs through just one objective, but detection of interfering light from the sample comes through both objective lenses [9], and thus its theoretical optical properties are identical to that of type-A 4Pi [10]. In type-C, both illumination and detection are of interfering light in the sample volume, through both objectives [8], permitting even greater resolution [10].

Resolution is best understood in the context of the axial optical transfer function (OTF), also called the  $z$ -response function. Qualitatively, the OTF shows the contribution to the detected light from different depths in the sample (i. e., points along the optical axis). An ideal microscope would have only light from a single point in the focal plane contributing to the detected signal; in that case, the OTF would be delta function at the focus of the microscope objective (Fig. 1.4(a)). In a regular confocal, instead of a single delta function, the effects of finite-sized illumination volume and imperfect pinhole discrimination combine to smear out the delta function into a nearly gaussian OTF (Fig. 1.4(b)); with 633 nm HeNe laser illumination, the OTF of a regular confocal has a full-width at half-maximum (FWHM) of 500 nm (theory and experiment) [10]. In 4Pi confocal microscopy, the counter propagating light waves of the same frequency and intensity that illuminate the sample create an interference pattern (a standing wave). Instead of a simply gaussian shape, the OTF now has one central peak and several so-called side-lobes (Fig. 1.4(c), (d)). The main advantage is that this central peak has a far narrower FWHM, theoretically calculated to be 130 nm for type-A (and thus for the optically equivalent type-B) and 95 nm for type-C, and measured at 140 nm and 95 nm, respectively [10]. The width of the central peak is independent of the relative phase between the two illuminating wavefronts (i. e., constructive or destructive interference are equivalent) [11], but nevertheless comes at the cost of having prominent side-

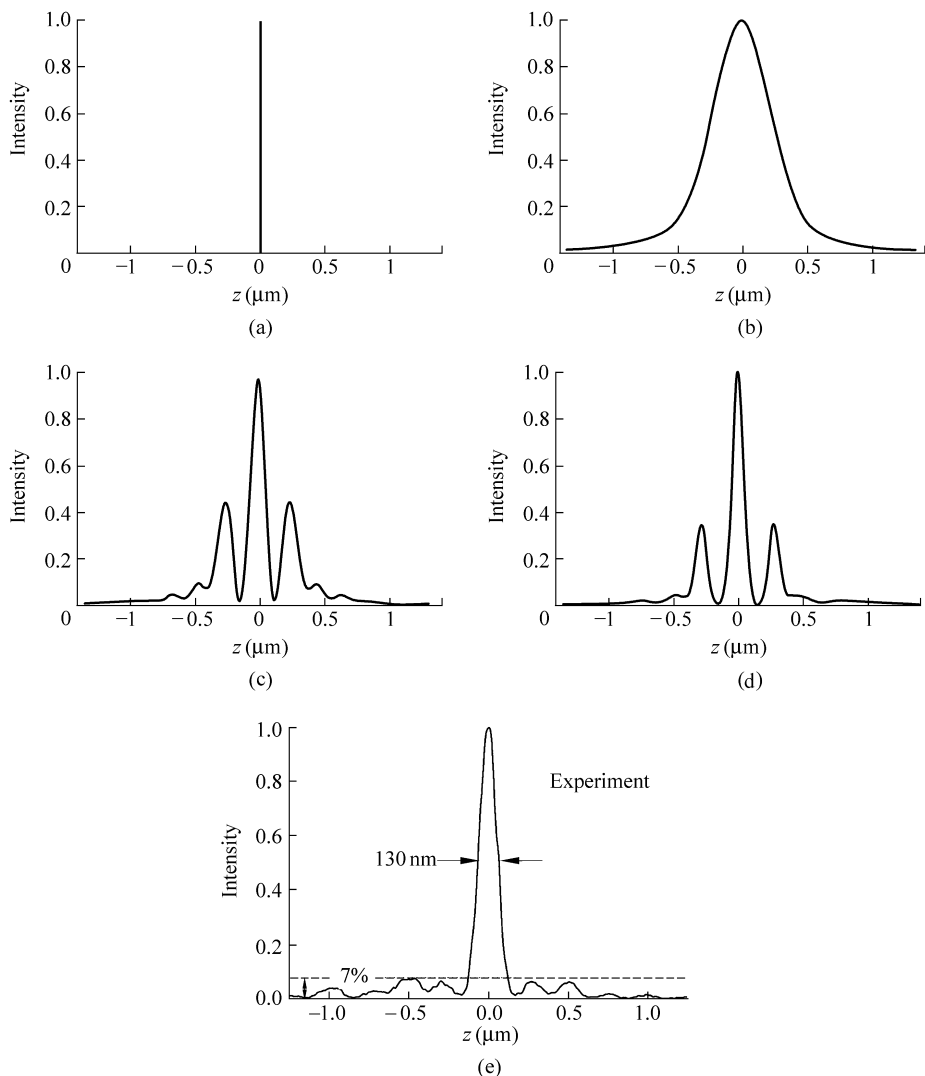


**Figure 1. 4**  $z$ -response functions for various types of microscopes: (a) ideal imaging system, with a deltafunction at  $z = 0$ , (b) typical confocal microscope, with a gaussian profile, (c) 4Pi-A microscope, (d) 4Pi-C microscope, (e) 4Pi-A with dark ring to reduce side lobes[8, 12]

lobes. That is, there is now a greater contribution to the light detected through the pinhole from some points farther away along the optic axis from the focal point than from some points closer, which creates artifacts. Almost all of the more recent technological developments in the 4Pi area have focused on optical tricks to eliminate the effects of those side bands: spatially filtering illuminating



light beams with specifically-placed dark rings[12, 13] or illuminating with two photons[14, 15] to cut off the light that contributes mainly to side lobes, and computational modeling of an ideal microscope to reconstruct an ideal image from real data in a process known as deconvolution[15 – 17]. Such techniques have yielded a confocal with an effective point-spread function with a width as small as 127 nm for a type-A 4Pi confocal, with no significant contribution from the side lobes (Fig. 1. 4(e)) [12], allowing sub-10 nm distances between test objects to be measured with uncertainties less than a single nanometer[18].

Such high resolution may finally allow direct imaging of nanoscale structures, and Leica Microsystems has just introduced the first commercial 4Pi system, the TCS 4Pi, in Apr 2004 (Fig. 1. 5). Nonetheless, there still remain some limitations to current 4Pi technology. The number of optical elements to be aligned and controlled in a 4Pi setup is at least twice that of a regular confocal, and since the stage is usually scanned in a 4Pi setup, scanning speeds are much lower, requiring minutes to image a full frame. While fast enough to image stationary samples like fixed cells[19], or even slow-moving live ones[20], this

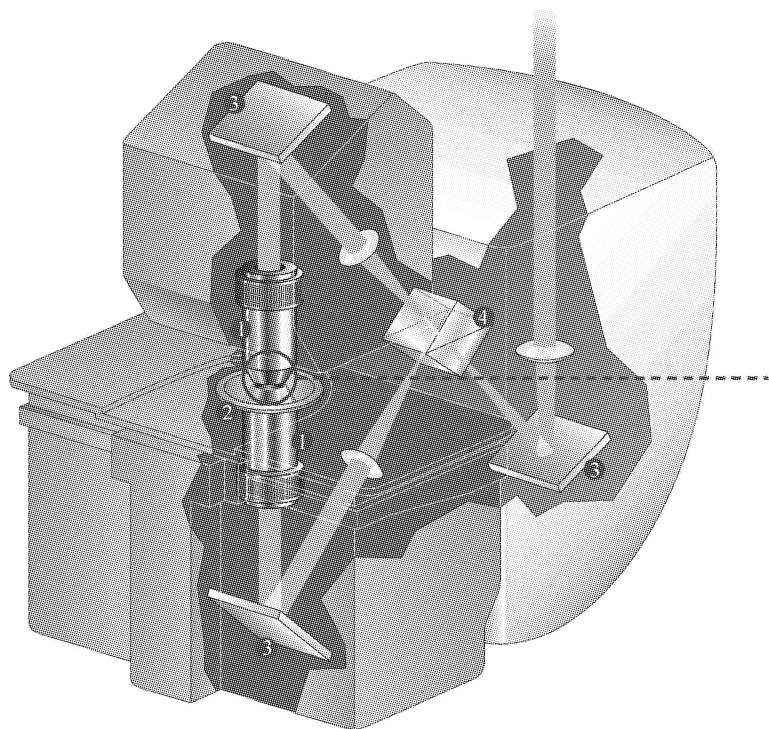


**Figure 1.5** Leica TCS 4Pi confocal microscope: (1) objective lenses, (2) sample holder, (3) mirrors, (4) beam splitter. Courtesy of Leica Microsystems, Heidelberg GmbH

is too slow to monitor most real-time dynamics at present, though scanning speed can be improved by using multiple beam scanning techniques in setups similar to the Nipkow disk, cutting imaging time down to seconds[21].

### 1.2.3.2 Other Optical Techniques to Increase Resolution

Several other far-field optical techniques have achieved high resolution without spatial filtering by means of a pinhole. As they are neither confocal techniques, nor have been widely applied to systems relevant to nanotechnology, they will receive only brief mention.

Removing the pinholes and illuminating with an incoherent (non-laser) source in the 4Pi-A, 4Pi-B and 4Pi-C geometries results in a setups known as  $I^3M$ ,  $I^2M$ , and  $I^5M$ , respectively[22, 23]. Compared with 4Pi, these widefield techniques show an equivalent increase in axial resolution, though the lateral resolution is not as great. The main advantage is collection speed: light is collected from the entire imaging plane at once, as there is no beam to be scanned. The major drawback is the requirement for a large amount of computationally intense deconvolution to obtain images. Other techniques have used different geometries, objectives, mirrors, or multiple photons for illumination, but none thus far has achieved better resolution than 4Pi or  $I^5M$ , and have not been applied widely to systems of interest to nanotechnology; an excellent survey comparing the techniques is given in Ref. [24].

A couple of non-traditional optical techniques have also increased resolution in novel ways. Placing a solid hemispherical lens against the surface of the sample (Fig. 1.6(a)) can improve resolution to a few times better than can be achieved with only a regular objective, with light collection efficiency improved five-fold. Interestingly, these improvements still persist even if the lens is slightly tilted, or there is a small air gap between the lens and the sample[25]. Also, common light detectors (photomultiplier tube, PMT; avalanche photodiode, APD; CCD) collect only intensity information, and can not measure phase directly. Interfering two beams, however, creates the a single output beam whose intensity is directly dependent on the phase difference of the two interfering beams. In practice, light can collected from two optical fibers (in place of the pinhole at the detector of the confocal), one along the optic axis, and one slightly displaced in the lateral direction. The signals from the two fibers are then interfered in a  $2 \times 1$  optical fiber coupler (Fig. 1.6(b)), which creates a single output beam whose intensity is measured. This interferometric technique is sensitive to single nanometer displacements on millisecond timescales[26]. Though not strictly an optical technique, another way to increase localization precision is to use objects that emit several colors. By detecting the different colors in separate channels, then combining the position data from different colors, the final position of the objects can be determined to an accuracy of better than 10 nm[27, 28]; the technique has also been used in 4Pi confocal setups [29] to achieve localization with single nanometer precision[30].

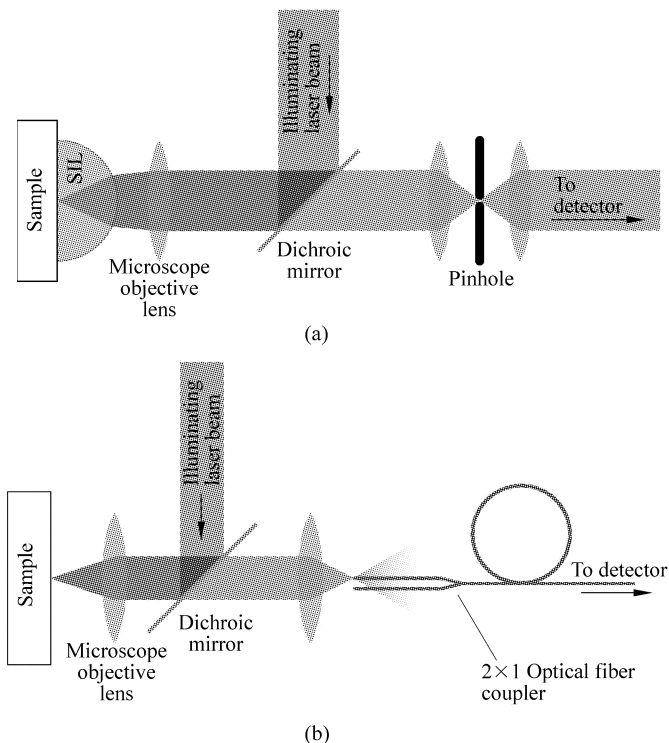


**Figure 1.6** other components to increase resolution: (a) solid immersion lens, placed up against the sample, and (b)  $2 \times 1$  optical coupler to interfere the light from the two fibers

### 1.3 Applications to Nanotechnology

As previously mentioned, the main contribution of confocal microscopy has not been to image nanoscale objects with light, but rather to use the capability to analyze the photons that have interacted with nanoscale structures, looking at their energies, temporal distribution, polarization, etc. As a result, the confocal can play a unique role in gathering information that can be obtained with no other technique. Many of the advances have come from the confocal's ability to characterize the properties of individual nanoscale objects, where previously only bulk ensemble averages could be measured. The discussion of how the confocal has been harnessed to gain information from nanoscale systems is organized by dimensionality of the system, in decreasing order.

## 1.3.1 Three-Dimensional Systems

### 1.3.1.1 Nanoemulsions

An emulsion is a mixture of two immiscible liquids: small droplets of the first liquid are dispersed in the second one, called the continuous phase. Such a mixture is intrinsically unstable, and droplets will coalesce unless a surfactant is added to the continuous phase. The surfactant helps to stabilize the interface between the two liquids by reducing the surface tension between them. Except in the case of microemulsions, emulsions are thermodynamically unstable [31]. Aging leads to a change in the size distribution of the droplets, and occurs via two mechanisms: coalescence, where smaller droplets combine to form larger ones, and Ostwald ripening, where larger droplets grow at the expense of smaller ones via diffusion of molecules through the continuous phase.

Confocal observation of the changing fluorescence intensity of single nanodroplets (as small as 50 nm) flowing through a capillary tube permitted investigation into the fundamental process of emulsion coarsening in a way not accessible to bulk measurement: the rate of drop growth could be measured for single nanoscale drops in the confocal, not a statistical average for the emulsion as a whole. The work demonstrated that Ostwald ripening and coalescence were occurring at different stages of emulsion coarsening [32], and dye diffusion was further studied by looking at fluorescence dynamics in mixtures of undyed and dyed emulsions [33]. Potential applications as isolated containers make nanoemulsions particularly interesting: encapsulation of a water-insoluble drug compound into the oil droplets of a nanoemulsion may allow controlled delivery of a substance to a designated target area in the body. Confocal has been used to monitor the uptake of dyed diblock copolymer nanoemulsions into cells [34], and the targeted delivery to cell organelles, each dyed a different color [35].

### 1.3.1.2 Nanocapsules

Nanocontainers can also be created by coating colloidal spheres, nanocrystals or other templates, then dissolving out the core to leave a rigid hollow shell, contrasting the soft surface of an emulsion. The templates have designable properties and are typically micron-sized; the term nanocapsule refers to the controllable organization of wall layers: starting with a charged core, layers of alternating charged polyelectrolytes can be deposited with nanometer thicknesses in a technique known as layer-by-layer (LBL) self-assembly. The chemistry of the polyelectrolytes can be varied significantly, and they can also serve as hosts for a variety of other materials, particularly ones with interesting photonic properties [36].

Confocal characterization has been used for real-time, three-dimensional

imaging of the growing nanocapsules and subsequent core dissolution in a number of systems: single-walled containers templated around a cadmium carbonate core [37], concentric sphere-in-sphere nanocapsules more mechanically robust than their single-wall counterparts[38], nanocapsules with silver ions in the walls for designable catalysis[39], biocompatible nanocapsules labeled with luminescent CdTe nanocrystals [40], and nanocapsules constructed by LBL assembly of dendrimers, large branching macromolecules with fractal structure[41].

Nanocapsules can also provide a controllable local environment for investigating nanoscale chemical reactions. LBL assembly and tuning the external environment allow very fine control over the permeability of the capsule to small molecules and ions, so that large enzyme molecules can be held inside nanocapsules whose walls are permeable to a fluorescent substrate [42]. By monitoring the fluorescence changes in real-time, the confocal gives a unique, quantitative, single-molecule view on enzyme activity [43], where previous techniques have only allowed bulk measurement of average activity; without the confocality, there is no way to isolate a single nanocapsule for study. Similarly, a pH gradient can be created between the inside and outside of a nanocapsule, and the confocal has monitored selective pH-induced precipitation of iron oxide nanocrystals inside single nanocapsules[44].

### 1.3.1.3 Other Three-Dimensional Nanostructures

The confocal's ability to spatially resolve spectral information in three dimensions has been used to characterize the nanostructure of other heterogenous materials. These systems may be constructed of different phases, such as the low-temperature Shpol'ski systems, where confocal spectroscopy was used to quantify preferential alignment of individual aromatic hydrocarbons molecules in a host of alkanes[45]. The confocal can also image the negative space in a porous material (e. g., nano-scale holes or pores) filled with dye, such as the spaces between layers of hydrotalcite-like compounds, including anionic clays and layered double hydroxides[46].

## 1.3.2 Two-Dimensional Systems

### 1.3.2.1 Ferroelectric Thin Films

Even in the absence of an external electric field, ferroelectric materials exhibit an electric dipole below a certain transition temperature, and they are the electric-field analog of a ferromagnet[47]. Above this transition temperature, the net electric dipole is no longer present, but ferroelectric materials still have a nonlinear dielectric constant useful for creating elements (such as capacitors and phase shifters) in microwave integrated circuits for insertion into wireless and satellite communications devices [48]. These materials, often based on the barium/strontium titanate (BST) perovskite structure, have different properties

whether in bulk or in a thin film.

Here, the confocal microscope has not contributed as a light-based imaging device in the traditional sense; rather, its capabilities to place a probing electric field precisely have been leveraged in a unique way to probe the physics of ferroelectrics[49 – 51]. First, pumping a BST thin film with a micron-scale capacitor aligns the film's molecular dipoles with an external electric field. After a controllable delay time, during which these dipoles begin to relax, the confocal microscope places a diffraction-limited spot of light at a particular location on the surface of a thin film. The electric field component of the illuminating laser beam serves as a sensitive probe, with emitted light having a different polarization or intensity as a result of its interaction with the ferroelectric material. Position and delay time are varied, with submicron and picosecond control. Changes in the emitted light from BST films grown under different pressures of oxygen suggest that reorientation of polarity on the nanoscale level is ultimately responsible for changes in ferroelectric behavior[52].

### **1.3.2.2 Nanopores, Nanoholes, and Nanomembranes**

The confocal has also been used to characterize the spatial distribution of negative space in two-dimensional systems, such as nanopores in titania thin film solar cell electrodes [53], luminescent conjugated polymers in nanoporous alumina [54], and pieces of fluorescently-labeled cell membrane stretched over nanoscale holes in silicon nitride[55]. This last technique is favored for AFM and other scanning-probe investigations of membranes, as isolated suspended membrane patches have improved stability and access relative to whole cells, and nanoholes are easily created with standard photolithography techniques. While SEM can characterize coverage of a cell membrane suspended over a nanohole, it is a two-dimensional technique that cannot discriminate between a suspended cell membrane and a pile of cell debris sitting on the silicon nitride surface. The three-dimensional sectioning ability of the confocal plays a critical role here: monitoring the height-dependence of fluorescence intensity yields a depth profile of fluorescent cell material, quickly distinguishing freely suspended cell membranes as small as 50 nm on a side[55].

## **1.3.3 One-Dimensional Systems**

### **1.3.3.1 Carbon Nanotubes**

The bulk processes (e. g. , carbon vapor deposition) that create carbon nanotubes typically yield a mixture of diameters, lengths, and structures, each with different physical properties. A major goal of nanoengineering is narrowing the distribution of sizes and structures to create materials with better-defined properties. Although the typical nanotube diameter of a few nanometers is well below the threshold of optical visibility, differences in nanotube structure

measurably change Raman spectral profiles. This confers upon the confocal a singularly important role in nanotube characterization, as its combination of spatial and spectral resolving capacity allow it to characterize individual nanotubes at speeds far greater than those accessible to other techniques. Characterizable attributes include nanotube diameter,  $(n, m)$  chirality[56, 57], and electrical conductivity [58], as well as distinguishing single-walled from multiple-walled[59], and free-standing from bundled nanotubes on insulating and conducting surfaces[60]. Confocal studies have been combined with AFM to better characterize the diameter-dependence of Raman peaks [58], and with HRTEM to precisely correlate atomic structure with spectral properties of the same nanotubes [61]. The confocal's high-speed, single nanotube characterization ability has also been harnessed as a screen in parallel microarray applications, including carbon vapor deposition on top of a microarray of different liquid catalysts to optimize synthesis[62], and a microarray constructed by linking DNA covalently to nanotubes to test sequence-specific binding interactions[63].

### 1.3.3.2 Nanowires

Confocal Raman spectroscopy has also characterized other one-dimensional systems. Raman spectra of silicon nanowires (5 – 15 nm) collected at low laser power match those of bulk silicon. But as power of the confocal's illuminating laser was increased, the Raman peaks shifted from those of bulk silicon in a way not consistent with quantum confinement effects, but rather suggesting that the laser is heating the wire itself[64].

### 1.3.4 Zero-Dimensional Systems

#### 1.3.4.1 Luminescent Nanocrystals (Quantum Dots)

Nanocrystals are crystals ranging in size from several nanometers to tens of nanometers, large enough so that single atoms do not drive their dynamics, while still small enough for their electronic and optical properties to be governed by quantum mechanical effects. Under confocal microscopy, where their size precludes resolution of their features, they effectively behave as zero-dimensional points. Of the common synonyms, including “nanoparticle” and “quantum dot”, only nanocrystal will be used here. The confocal has been used in two broad areas: spectrally characterizing individual nanocrystals, where confocality is required to isolate individual particles, and localizing nanocrystals as point tracers in other systems, utilizing the capability of three-dimensional, real-time localization.

Recent examples of confocal characterization of the energy spectra of individual nanocrystals include cryogenic (20 K) imaging of single 7-nm ZnS nanocrystals[65], and characterization of the optical extinction properties of

nanocrystals created by conventional nanosphere lithography [66]. Quantifying the temporal dynamics of the intermittent fluorescence (blinking) typical of nanocrystals yields information on their electronic structure, and the fast on-and-off fluorescence can be captured with high-speed optical detectors, like PMT or APD, attached to the confocal. Studies of individual CdSe nanocrystals overcoated with ZnS have shown that several energy levels may drive the optical behavior [67, 68], with similar results found for InP nanocrystals [69]. Measuring energy spectra over time has quantified changes due to oxidation of nanocrystals in air (versus no change in pure nitrogen) [70], and the size and surface-property dependence of the behavior of silicon quantum dots, both porous [71] and crystalline stabilized with an organic monolayer [72]. By splitting the light coming back from the sample, sending half to an APD and the remainder through a prism onto a CCD, high resolution time and spectral data can be collected simultaneously. This analysis, in combination with TEM of the same individual nanocrystals to correlate optical properties with atomic structure, has shown that a single crystalline domain is not required to achieve fluorescence [73]. Finally, to characterize the heavy dependence of fluorescence behavior on nearby conductors, confocal microscopy imaged a fluorescent dye attached to both bulk gold and gold nanocrystals on the same substrate. While the dye attached to bulk gold was quenched, since the energy absorbed by the fluorophore gets transferred to the sea of electrons in the metal, dyes attached to nanocrystals remained bright, as there is no bulk into which to transfer electrons [74].

The confocal has also been used to localize nanocrystals embedded in other systems. This has aided synthesis of organic nanocrystals grown in inorganic sol-gel coatings, with confocal characterization of their size and distribution allowing systematic exploration of the phase space of the main synthesis parameters [75]. Embedding nanocrystals within polyelectrolyte layers in LBL assembly allows nanometer control of thin-film coatings that can be applied to three-dimensional objects of complex geometry, whose luminescent properties are then determined by the nanocrystals. Three-dimensional sectioning in the confocal has been crucial to characterizing these coatings, which have been applied to cylindrical optical fibers [76] and spherical latex colloidal particles [77]. In addition, the confocal has been used to characterize the three-dimensional structure of micron-sized domains of nanocrystals, including silver nanocrystals embedded between two layers in a thin film and coalesced by irradiation with a high-intensity laser beam to create planar diffractive and refractive micro-optics [78], and silicon nanocrystals patterned onto surfaces by directing a stream of silicon atoms through a mask for nanofabrication of light sources from all silicon with pre-existing tools from the electronics industry [79].

In addition to these static applications, the real-time imaging capability of the confocal is useful for monitoring nanocrystal dynamics at higher speeds. Confocal microscopy has been combined with flow cytometry to image and count fluorescent nanoparticles in a fluid flow, yielding real-time information on their concentration [80]. Fluorescent colloidal nanospheres have been coated on one



side with gold, yielding an opaque hemispherical metal coating that appears dark, and floated on the surface of a liquid. Light intensity levels of individual nanospheres can be correlated with angular orientation, allowing real-time imaging of Brownian rotational diffusion to study molecular interactions, particularly the preferential attraction of fluid molecules toward one hemisphere over the other[81]. Metal oxide nanocrystals and their halogen adducts have been shown to kill bacteria, and a combination of confocal microscopy and electrostatic measurements has demonstrated that the particles and bacteria attracted each other on account of their electric charge, shedding light on nanoscale electrostatics in solution[82]. Finally, the active transport of single nanocrystals by a dynein motor protein along microtubules in live cells has been imaged in real time with a Nipkow disk confocal; interestingly, contrasting the blinking typical of nanocrystals in free solution, these nanocrystals in live cells have nearly constant intensity[83].

### 1.3.4.2 Viruses

Far-field confocal microscopy has been combined with a scanning near-field ion microscopy in water, with a micropipette carrying an ion current tens of nanometers from an optically invisible cell membrane surface to map topography. This technique has been used to image virus-like particles, nanospheres composed of a few hundred viral proteins enclosing DNA and their absorption into cells. The biological motivation is to understand how viruses infect living cells, but more generally, the investigation demonstrates confocal three-dimensional, real-time localization of a nanoscale object relative to an optically invisible surface[84].

By manipulating the genetic code of viruses, proteins on their surfaces can be modified to achieve desired properties in a technique called phage display, which early on was used to optimize highly-specific binding of viruses to a variety of semiconductor surfaces[85]. More recently, phage display has been used to control the morphology of calcium carbonate crystals precipitated from solution in the presence of viruses that template the crystals, in an effort to better understand biomineralization. While scanning electron microscopy can image and characterize the inorganic calcium carbonate after growth was stopped, confocal microscopy allowed three-dimensional localization of the fluorescently-labeled viruses relative to the growing crystals[86].

### 1.3.4.3 Single Molecule Studies

Confocal studies of single molecules fall into two broad groups: spectral characterization of single molecules and localization of fluorescent molecules as tags. Static single molecule systems characterized include individual dye molecules over a range of temperatures from liquid helium to room temperature [87], and optimized mutations of the fluorescent protein GFP in various three-dimensional substrates [88]; dynamically, time-correlation spectroscopy in the

confocal has been used to measure solution concentrations down to  $10^{-15}$  M[89]. While confocality may not be strictly necessary for these studies, increased resolution helps to isolate individual molecules. The confocal has also been used for three-dimensional localization of single fluorescent dye molecules attached as tags to another object of interest, such as single molecules inside a living cell [90], or correlating emission spectra of molecules on a mica substrate with AFM data to develop a way measure topography optically[91].

## 1.4 Summary and Future Perspectives

Confocal microscopy extends the characterization of ever smaller objects with optical microscopy to the nanometer scale. By using a pinhole to restrict detected light to only that coming from the focus of the microscope objective, the confocal allows three-dimensional sectioning and localization, often at rapid rates with proper scanning techniques. Spatially resolved spectroscopy has allowed investigation of a broad variety of systems of interest to nanotechnology, providing information accessible to no other technique.

Further developments may be anticipated in several areas. 4Pi-C confocal has already achieved resolution in the sub-100 nm range that defines “nanoscale”; it is possible that novel optical techniques will improve this even further. Other evolutionary engineering improvements will surely increase speed, perhaps allowing real-time 4Pi imaging comparable to regular confocal by using beam parallelization in the same spirit as the Nipkow disk.

The capabilities of the confocal to answer new kinds of questions are also being developed rapidly, in no small part due to the low cost and relative ease of construction of off-the-shelf laboratory optical components used to build instrumentation ancillary to the confocal. A large fraction of the applications described in this review utilized some form of home-built hardware, a trend which will surely continue. Spectroscopy will likely become faster, allowing the characterization of the changes in spectra on shorter timescales, with the ultimate goal of studying changes in single molecules, a new field with some early applications described. Better understanding of the behavior of isolated nanoscale objects will use the confocal microscope’s three-dimensional, real-time localization capability to study not only the dynamics of single particles, but also the behavior of systems of thousands, or perhaps even millions, of particles with controllable interactions. Clearly, the unique capabilities of the confocal microscope will ensure its contribution to the development of nanotechnology for the foreseeable future.

## References

- [1] Hooke, R. *Micrographia*. Royal Society, London(1667)
- [2] Brown, R. *A Brief Account of Microscopical Observations Made in the Months of June,*

*July and August 1827 on the Particles Contained in the Pollen of Plants; and on the General Existence of Active Molecules in Organic and Inorganic Bodies.* Taylor, London (1828)

- [3] Born, M. and E. Wolf. *Principles of optics : electromagnetic theory of propagation, interference and diffraction of light, 6th corr.* Oxford Cambridge University Press, New York(1997) p. 808
- [4] Sheppard, C. J. R. and D. M. Shotton. *Confocal Laser Scanning Microscopy.* BIOS Scientific Publishers, Oxford(1997)
- [5] Corle, T. R. and G. S. Kino. *Confocal Scanning Optical Microscope and Related Imaging Systems.* Academic Press, San Diego(1996)
- [6] Diaspro, A. *Confocal and Two-Photon Microscopy: Foundations, Applications, and Advances.* Wiley-Liss, New York(2002)
- [7] Gu, M. *Principles of Three-Dimensional Imaging in Confocal Microscopes.* World Scientific, Singapore(1996)
- [8] Hell, S. W. and E. H. H. Stelzer. Properties of a 4Pi confocal fluorescence microscope. *J. Opt. Soc. Am. A* **9**(12): 2159 – 2166(1992)
- [9] Hell, S. W. et al. Confocal microscopy with an increased detection aperture: type-B 4Pi confocal microscopy. *Optics Letters* **19**(3): 222 – 224( 1994)
- [10] Schrader, M. et al. Optical transfer functions of 4Pi confocal microscopes: theory and experiment. *Optics Letters* **22**(7): 436 – 438(1997)
- [11] Hell, S. W. and M. Nagorni. 4Pi confocal microscopy with alternate interference. *Optics Letters* **23**(20): 1567 – 1569(1998)
- [12] Blanca, C. M. and S. W. Hell. Sharp spherical focal spot by dark ring 4Pi-confocal microscopy. *Single Mol.* **2**(3): 207 – 210(2001)
- [13] Blanca, C. M., J. Bewersdorf and S. W. Hell. Determination of unknown phase difference in 4Pi-confocal microscopy through the image intensity. *Optics Communications* **206**: 281 – 285(2002)
- [14] Hell, S. W. and E. H. H. Stelzer. Fundamental improvement of resolution with a 4Pi-confocal fluorescence microscope using two-photon emission. *Optics Communications* **93** (5 – 6): 277 – 282(1992)
- [15] Soini, J. T. et al. Image formation and data acquisition in a stage scanning 4Pi confocal fluorescence microscope. *Applied Optics* **36**(34): 8929 – 8932(1997)
- [16] Schrader, M., S. W. Hell and H. T. M. van der Voort. Potential of confocal microscopes to resolve in the 50 – 100 nm range. *Applied Physics Letters* **69**(24): 3644 – 3646(1996)
- [17] Schrader, M., S. W. Hell and H. T. M. van der Voort. Three-dimensional super-resolution with a 4Pi-confocal microscope using image restoration. *Journal of Applied Physics* **84**(8): 4033 – 4042(1998)
- [18] Albrecht, B. et al. Spatially modulated illumination microscopy allows axial distance resolution in the nanometer range. *Applied Optics* **41**(1): 80 – 87(2002)
- [19] Schrader, M. et al. 4Pi-confocal imaging in fixed biological specimens. *Biophysical Journal* **75**: 1659 – 1668(1998)
- [20] Bahlmann, K., S. Jakobs and S. W. Hell. 4Pi-confocal microscopy of live cells. *Ultramicroscopy* **87**: 155 – 164(2001)
- [21] Egner, A., S. Jakobs and S. W. Hell. Fast 100-nm resolution three-dimensional microscope reveals structural plasticity of mitochondria in live yeast. *Proceedings of the National Academy of Sciences* **99**(6): 3370 – 3375(2002)
- [22] Gustafsson, M. G. L. Surpassing the lateral resolution limit by a factor of two using structured illumination microscopy. *Journal of Microscopy* **198**(2): 82 – 87(2000)

- [23] Gustafsson, M. G. L., D. A. Agard and J. W. Sedat. I5M: 3D widefield light microscopy with better than 100 nm axial resolution. *Journal of Microscopy* **195**(1): 10 – 16(1999)
- [24] Gustafsson, M. G. L. Extended resolution fluorescence microscopy. *Current Opinion in Structural Biology* **9**: 627 – 634(1999)
- [25] Moehl, S. et al. Solid immersion lens-enhanced nano-photoluminescence: principle and applications. *Journal of Applied Physics* **93**(10): 6265 – 6272(2003)
- [26] Bae, J. H. et al. High resolution confocal detection of nanometric displacement by use of a  $2 \times 1$  optical fiber coupler. *Optics Letters* **25**(23): 1696 – 1698(2000)
- [27] Lacoste, T. D. et al. Ultrahigh-resolution multicolor colocalization of single fluorescent probes. *Proceedings of the National Academy of Sciences* **97**(17): 9461 – 9466(2000)
- [28] Michalet, X., T. D. Lacoste and S. Weiss. Ultrahigh-resolution colocalization of spectrally separable point-like fluorescent probes. *Methods* **25**: 87 – 102(2001)
- [29] Kano, H. et al. Dual-color 4-Pi confocal microscopy with 3D-resolution in the 100 nm range. *Ultramicroscopy* **90**: 207 – 213(2002)
- [30] Schmidt, M., M. Nagorni and S. W. Hell. Subresolution axial distance measurements in far-field fluorescence microscopy with precision of 1 nanometer. *Review of Scientific Instruments* **71**(7): 2742 – 2745(2000)
- [31] Safran, S. *Statistical Thermodynamics of Surfaces, Interfaces and Membranes*. 1994, Boulder: Westview, 1994
- [32] Sakai, T. et al. Monitoring growth of surfactant-free nanodroplets dispersed in water by single-droplet detection. *Journal of Physical Chemistry B* **107**: 2921 – 2926(2003)
- [33] Sakai, T. et al. Dye transfer between surfactant = free nanodroplets dispersed in water. *Journal of Physical Chemistry B* **106**: 5017 – 5021(2002)
- [34] Nam, Y. S. et al. New micelle-like polymer aggregates made from PEI-PLGA diblock copolymers: micellar characteristics and cellular uptake. *Biomaterials* **24**: 2053 – 2059 (2003)
- [35] Savic, R. et al. Micellar nanocontainers distribute to defined cytoplasmic organelles. *Science* **300**: 615 – 618(2003)
- [36] Decher, G. Fuzzy nanoassemblies: toward layered polymeric multicomposites. *Science* **277**: 1232 – 1237(1997)
- [37] Silvano, D. et al. Confocal laser scanning microscopy to study formation and properties of polyelectrolyte nanocapsules derived from  $\text{CdCO}_3$  templates. *Microscopy Research and Technique* **59**: 536 – 541( 2002)
- [38] Dai, Z. et al. Nanoengineering of polymeric capsules with a shell-in-shell structure. *Langmuir* **18**: 9533 – 9538(2002)
- [39] Antipov, A. A. et al. Fabrication of a novel type of metallized colloids and hollow capsules. *Langmuir* **18**: 6687 – 6693(2002)
- [40] Gaponik, N. et al. Labeling of biocompatible polymer microcapsules with near-infrared emitting nanocrystals. *Nano Letters* **3**(3): 369 – 372(2003)
- [41] Khopade, A. J. and F. Caruso. Electrostatically assembled polyelectrolyte/dendrimer multilayer films as ultrathin nanoreservoirs. *Nano Letters* **2**(4): 415 – 418(2002)
- [42] Lvov, Y. et al. Urease encapsulation in nanoorganized microshells. *Nano Letters* **1**(3): 125 – 128(2001)
- [43] Chiu, D. T. et al. Manipulating the biochemical nanoenvironment around single molecules contained within vesicles. *Chemical Physics* **247**: 133 – 139(1999)
- [44] Radtchenko, I. L., M. Giersig and G. B. Sukhorukov. Inorganic particle synthesis in confined micron-sized polyelectrolyte capsules. *Langmuir* **18**: 8204 – 8208(2002)
- [45] Bloess, A. et al. Microscopic structure in a shpol' skii system: a single-molecule study

of dibenzanthanthrene in n-tetradecane. *Journal of Physical Chemistry A* **105**: 3016 – 3021(2001)

- [46] Latterini, L. et al. Space-resolved fluorescence properties of pheolphthalein-hydrotralcie nanocomposites. *Phys. Chem. Chem. Phys.* **4**: 2792 – 2798(2002)
- [47] Kittel, C. *Introduction to Solid State Physics*. 7th ed. Wiley, New York(1996)
- [48] Van Keuls, F. W. et al. A Ku-band gold/BaxSr1-xTiO<sub>3</sub>/LaAlO<sub>3</sub> conductor/thin film ferroelectric microstrip line phase shifter for room-temperature communications applications. *Microwave and Optical Technology Letters* **20**(1): 53 – 56(1999)
- [49] Hubert, C. and J. Levy. New optical probe of GHz polarization dynamics in ferroelectric thin films. *Review of Scientific Instruments* **70**(9): 3684 – 3687(1999)
- [50] Hubert, C. et al. Confocal scanning optical microscopy of BaxSr1-xTiO<sub>3</sub> thin films. *Applied Physics Letters* **71**(23): 3353 – 3355(1997)
- [51] Hubert, C. et al. Mesoscopic microwave dispersion in ferroelectric thin films. *Physical Review Letters* **85**(9): 1998 – 2001(2000)
- [52] Hubert, C. et al. Nanopolar reorientation in ferroelectric thin films. 2001
- [53] Tesfamichael, T. et al. Investigations of dye-sensitised titania solar cell electrode using confocal laser scanning microscopy. *Journal of Materials Science* **38**: 1721 – 1726(2003)
- [54] Qi, D. et al. Optical emission of conjugated polymers adsorbed to nanoporous alumina. *Nano Letters* **3**: (2003)
- [55] Fertig, N. et al. Stable integration of isolated cell membrane patches in a nanomachined aperture. *Applied Physics Letters* **77**(8): 1218 – 1220(2000)
- [56] Jorio, A. et al. Structural (n, m) determination of isolated single-wall carbon nanotubes by resonant Raman scattering. *Physical Review Letters* **86**(6): 1118 – 1121(2001)
- [57] Azoulay, J. et al. Polarised spectroscopy of individual single-wall nanotubes: Radial-breathing mode study. *Europhysics Letters* **53**(3): 407 – 413(2001)
- [58] Zhao, J. et al. Diameter-dependent combination modes in individual single-walled carbon nanotubes. *Nano Letters* **2**(8): 823 – 826(2002)
- [59] Ecklund, P. C. et al. Large-scale production of single-walled carbon nanotubes using ultrafast pulses from a free electron laser. *Nano Letters* **2**(6): 561-566(2002)
- [60] Sangaletti, L. et al. Carbon nanotube bundles and thin layers probed by micro-Raman spectroscopy. *The European Physical Journal B* **31**: 203 – 208(2003)
- [61] Jiang, C. et al. Combination of confocal Raman spectroscopy and electron microscopy on the same individual bundles of single-walled carbon nanotubes. *Nano Letters* **2**(11): 1209 – 1213(2002)
- [62] Chen, B. et al. Heterogeneous single-walled carbon nanotube catalyst discovery and optimization. *Chem. Mater.* **14**: 1891 – 1896(2002)
- [63] Hazani, M. et al. Confocal fluorescence imaging of DNA-functionalized carbon nanotubes. *Nano Letters* **3**(2): 153-155(2003)
- [64] Gupta, R. et al. Laser-induced fano resonance scattering in silicon nanowires. *Nano Letters* **3**(5): 627 – 631(2003)
- [65] Tittel, J. et al. Fluorescence spectroscopy on single CdS nanocrystals. *J. Phys. Chem. B.* **101**(16): 3013 – 3016(1997)
- [66] Haynes, C. L. and R. P. van Duyne. Dichroic optical properties of extended nanostructures fabricated using angle-resolved nanosphere lithography. *Nano Letters* **3** (7): 939 – 943(2003)
- [67] Kuno, M. et al. Nonexponential “blinking” kinetics of single CdSe quantum dots: A universal power law behavior. *Journal of Chemical Physics* **112**(7): 3117 – 3120( 2000)
- [68] Kuno, M. et al. “On”/“off” fluorescence intermittency of single semiconductor quantum dots. *Journal of Chemical Physics* **115**(2): 1028 – 1040(2001)

- [69] Kuno, M. et al. Fluorescence intermittency in single InP quantum dots. *Nano Letters* **1** (10): 557 – 564(2001)
- [70] van Sark, W. G. J. H. M. et al. Photooxidation and photobleaching of single CdSe/ZnS quantum dots probed by room-temperature time-resolved spectroscopy. *J. Phys. Chem. B* **105**: 8281 – 8284(2001)
- [71] Mason, M. D. et al. Luminescence of individual porous Si chromophores. *Physical Review Letters* **80**(24): 5405 – 5408(1998)
- [72] English, D. S. et al. Size tunable visible luminescence from individual organic monolayer stabilized silicon nanocrystal quantum dots. *Nano Letters* **2**(7): 681 – 685 (2002)
- [73] Koberling, F. et al. Fluorescence spectroscopy and transmission electron microscopy of the same isolated semiconductor nanocrystals. *Applied Physics Letters* **81**(6): 1116 – 1118( 2002)
- [74] Levi, S. A. et al. Fluorescence of dyes adsorbed on highly organized, nanostructured gold surfaces. *Chem. Eur. J.* **8**(16): 3808 – 3814(2002)
- [75] Sanz, N. et al. Organic nanocrystals grown in sol-gel coatings. *Journal of Materials Chemistry* **10**: 2723 – 2726(2000)
- [76] Crisp, M. T. and N. A. Kotov. Preparation of nanoparticle coatings on surfaces of complex geometry. *Nano Letters* **3**(2): 173 – 177(2003)
- [77] Susha, A. S. et al. Formation of luminescent spherical core-shell particles by the consecutive adsorption of polyelectrolyte and CdTe(S) nanocrystals on latex colloids. *Colloids and Surfaces A: Physicochemical and Engineering Aspects* **163**: 39 – 44(2000)
- [78] Martin, J. et al. Laser microstructuring and scanning microscopy of plasmapolymer-silver composite layers. *Applied Optics* **40**(31): 5726 – 5730(2001)
- [79] Ledoux, G. et al. Nanostructured films composed of silicon nanocrystals. *Materials Science and Engineering C* **19**: 215 – 218(2002)
- [80] Ferris, M. M. and K. L. Rowlen. Detection and enumeration of single nanometric particles: A confocal optical design for fluorescence flow cytometry. *Review of Scientific Instruments* **73**(6): 2404 – 2410(2002)
- [81] Choi, J. et al. Patterned fluorescent particles as nanoprobes for the investigation of molecular interactions. *Nano Letters* **3**(8): 995 – 1000(2003)
- [82] Stoimenov, P. K. et al. Metal oxide nanoparticles as bactericidal agents. *Langmuir* **18**: 6679 – 6686(2002)
- [83] Chen, P. et al. High imaging sensitivity and blinking suppression of single quantum dots in a live cell: visualization of dynein mediated active transport at the video rate. *Nature Biotechnology*(2004)
- [84] Gorelik, J. et al. Scanning surface confocal microscopy for simultaneous topographical and fluorescence imaging: Application to single virus-like particle entry into a cell. *Proceedings of the National Academy of Sciences* **99**(25): 16,018 – 16,023(2002)
- [85] Whaley, S. R. et al. Selection of peptides with semiconductor binding specificity for directed nanoparticle assembly. *Nature* **405**: 665 – 668(2000)
- [86] Li, C., G. D. Botsaris and D. L. Kaplan. Selective in vitro effect of peptides on calcium carbonate crystallization. *Crystal Growth and Design* **2**(5): 387 – 393(2002)
- [87] Segura, J.-M., A. Renn and B. Hecht. A sample-scanning confocal optical microscope for cryogenic operation. *Review of Scientific Instruments* **71**(4): 1706 – 1711(2000)
- [88] Chirico, G. et al. Dynamics of green fluorescent protein mutant 2 in solution, on spin-coated glasses, and encapsulated in wet silica gels. *Protein Science* **11**: 1152 – 1161 (2002)
- [89] Nie, S. and R. N. Zare. Optical detection of single molecules. *Annual Reviews of*

Biophysics and Biomolecular Structure **26**: 567 – 596(1997)

- [90] Byassee, T. A. , W. C. W. Chan and S. Nie. Probing single molecules in single living cells. *Analytical Chemistry* **72**(22): 5606 – 5611(2000)
- [91] Kolody, L. A. et al. Spatially correlated fluorescence/AFM of individual nanosized particles and biomolecules. *Analytical Chemistry* **73**(9): 1959 – 1966(2001)

---

The author would like to thank I. Cohen, L. Kaufman, N. Tsapis and E. Dufresne for comments on the manuscript, and B. Calloway of Leica Microsystems for providing Fig. 1. 5.